 doi:10.20944/preprints202203.0308.v1

Article

Laser Structuring and DLC Coating of Elastomers for High Performance Applications

Sönke Vogel [1]*, Andreas Brenner [2], Bernadette Schlüter [3], Bernhard Blug [4], Franziska Kirsch [5] and Tamara van Roo[6]

[1] Chair for Laser Technology LLT, RWTH Aachen University, Aachen; soenke.vogel@llt.rwth-aachen.de
[2] Fraunhofer Institute for Laser Technology, Aachen; andreas.brenner@ilt.fraunhofer.de
[3] Fraunhofer Institute for mecanics of materials, Freiburg; bernadette.schlueter@iwm.fraunhofer.de
[4] Fraunhofer Institute for mecanics of materials, Freiburg; bernhard.blug@iwm.fraunhofer.de
[5] Fraunhofer Institute for Structural Durability and System Reliability LBF, Darmstadt; franziska.kirsch@lbf.fraunhofer.de
[6] Fraunhofer Institute for Structural Durability and System Reliability LBF, Darmstadt; tamara.van.roo@lbf.fraunhofer.de
* Correspondence: soenke.vogel@llt.rwth-aachen.de

Abstract: Even though hard, low friction coatings such as diamond like carbon (DLC) would be beneficial for the performance and longevity of rubber seals, a crucial challenge – as graphically illustrated in Figure 1.a – remains. The elastic mismatch of rubber substrate and DLC coating prevents a fracture free coating application. In this work a nature inspired approach (Figure 1.b) is applied to render the stiff coating flexible and resilient to delamination at the same time by direct patterning. Rubber substrates were laser structured with tile patterns and subsequently DLC-coated. Tensile and tribology tests were performed on structured and unstructured samples. Unstructured DLC-coatings showed a crack pattern induced by the coating process, which was further fragmented by tensile stress. Coatings with tile patterns did not experience a further fragmentation under load. During continuous tribological loading, less heterogenous damage is produced for tile structured samples. The findings are ascribed to the relief of induced coating stress by the tile structure, meaning a more resilient coating.

(**a**) (**b**)

Figure 1. Ice floes on water as analogy for a stiff Diamond Like Carbon film on an elastic substrate (a) and a nature inspired improvement of the film-substrate system. © Marcus Löfvenberg (a) and Photo by David Clode (b) on Unsplash.

Keywords: diamond like carbon, DLC, Tribology, rubber, flexible, nature inspired, coating, friction, sealing, delamination

 doi:10.20944/preprints202203.0308.v1

1. Introduction

Rubber seals are everywhere. And in every dynamic seal the rubber is responsible 50 – 70 % of friction losses. A hard, protecting, and low friction coating such as diamond like carbon (DLC) would significantly enhance the performance of dynamic rubber seals. Besides the already mentioned properties of DLC, good adhesion and flexibility are mandatory requirements. Whereas the coefficient of friction (CoF) reduction of DLC coatings compared to their pristine substrate has been shown [1–7], the latter properties are subject to ongoing research. Especially the microstructure of the DLC film is has been attributed to adhesion and flexibility performance [6–9]. As graphically illustrated in Figure 1, an ice floe pattern is inherent to the coating process resulting from a thermal coefficient mismatch of substrate and coating. Hence, the stiffer DLC-coating is prone to the formation of buckling cracks. A dense crack pattern with small patches was found to enhance the adhesion [6] and flexibility [10]. The microstructure was related to substrate hardness [4] ,surface chemistry and roughness [6,11] as well as coating conditions with preceding plasma treatment [5,7–9,12]. The latter method aims to passively influence the microstructure and is thus regarded as a subtype of microstructuring. Direct microstructuring was performed with a net mask. However, the tested substrate was "soft" aluminum and the smallest achievable patch size was 1 mm with 100 µm spacing [13], whereas patch sizes below 60 µm were found to unify good adhesion and CoF [7,9,12].

The primordial crack pattern of native coatings is formed by buckling and is crucial for attaining a flexible film. Under thermally induced compression, the coating either forms a blister and finally cracks at the blister ridge [14,15] or it wrinkles in a complex sinusoidal pattern and cracks at the trench [16,17]. The latter was found for DLC-coatings on compliant substrates [18] and is unavoidable in natively grown films. However, the film is prone to crack further under load and debris is generated [5,6,9,11].

In this study we aim to control the patch size – which has been identified as the most influential parameter – by direct ultrashort pulse (USP) laser microstructuring of the substrate. Whereas the native microstructure is only indirectly controllable and still strongly dependent on many influential parameters, a direct patterning could be beneficial in several ways: First, the tribological properties of the film could be further enhanced by microstructures. Second, the microstructures could act as a lubricant reservoir. Third, the adhesion and flexibility could be improved further in comparison to passively controlled native films.

We hypothesize that the proposed tile pattern is believed to surpass passively controlled films with regards to delamination performance. The tile pattern is expected to suppress wrinkling and fragmentation during loading, resulting in smoother, long-term stable coatings. We did not aim to optimize the dimensions of the tile pattern to obtain a lower CoF. This study focuses on the long-term adhesion of the coating which is reflected by a smaller change of the CoF compared to an unstructured sample.

2. Materials and Methods

2.1. Materials

Nitrile-Butadien-Rubber (NBR) and Fluorelastomers (FKM) are the most common materials for sealing applications. To address as much sealing applications as possible both ,NBR and FKM with different hardness (Shore A), are investigated. Furthermore, two different kinds of Styrene-ethylene-butylene-styrene (SEBS) are examined as an example of thermoplastic elastomers Table 1 shows the materials used and their ShoreA-hardness if measured.

Preprints (www.preprints.org) | NOT PEER-REVIEWED | Posted: 23 March 2022 doi:10.20944/preprints202203.0308.v1

Table 1. Threshold Fluences F_{Th}, Shore Hardnesses and visual appearances of rubbers used in this study.

Rubber	Manufacturer	Hardness [°ShA]	Visual Appearance	F_{Th} [Jcm^{-2}]
FKM *803915.3*	DuPont Performance Elastomere	75	black	0.79
FKM *803927.4*	Freudenberg Sealing Technologies	64	black	0.75
NBR *802607.2*	Freudenberg Sealing Technologies	76	black	1.53
NBR *804506.1*	Goorex	70	black	1.82
SEBS *G1650*	Freudenberg Sealing Technologies	70	translucent	0.89
SEBS *H1062*	Freudenberg Sealing Technologies	77	translucent	0.99

2.2. *Laser Processing*

The rubbers were processed with ultra-short laser pulses (USP) utilizing a PHAROS (LightConversion, Lithuania) system with a repetition rate of 200 kHz, 200 fs pulse width at a central wavelength of 343 nm. Three different surface topographies were engraved:

1. Tile pattern with a hatch distance of 60 µm and a trench width and depth of 10 µm and 30 µm, respectively. In the further text referred to as S1.
2. Tile pattern with a hatch distance of 30 µm and a trench width and depth of 10 µm (S2)
3. Single depressions distanced by 20 µm in two perpendicular directions with a diameter and depth of 10 µm (S3).

All trenches were processed with a spatial pulse overlap of 75 % and all depressions by a spatial overlap of 100 % and 50 pulses. The trench depth and width were verified by cross sections. All microscope investigations utilized a VHX5000 (Keyence, Japan).

2.3. *DLC (a-C:H) -Coating of Rubber Substrates*

The samples were cleaned in an ultrasonic bath in ethanol. The samples were then DLC coated in a standard capacity coupled phyical enhanced physical vapor deposition plasma process (CCP PE-CVD) at a frequency of 13.56 MHz. The process started with a 5 min plasma cleaning in argon (35 SCCM) followed by a 2 min adhesion layer coating with tetramethylsilane (TMS, 17 SCCM) as precursor gas. The main coating gas (toluene) was then ramped for 5 min into the gas mixture by substituting the TMS by toluene. The power in the process was held constant at 200 W and the end pressure reached in the toluene process was 2.3 Pa.

2.4. *Tensile Tests*

All quasistatic tensile tests were executed on a servo-hydraulic Zwick/Roell testing machine equipped with a 20 kN load cell at constant velocity of 6 mm/min. The tensile tests were performed on unstructured, uncoated as well as coated FKM Viton 75 samples. Magnified images (x100) of the coated surface were taken for different strains during the first elongation. The strain information was evaluated by optical gray scale correlation (VIC2D, Correlated Solutions®). The initial length and width were both 12 mm. The length, width and transition radius are 80 mm, 20 mm and 20 mm, respectively.

The spatial frequency distribution (SPD) was obtained from the region in the range of |45°| along the elongation axis (see Appendix A for further calculations). It was assumed that crack formation due to tensile stress in the DLC coating is oriented preferentially perpendicular to the elongation direction. Therefore, a shift of the SPD to shorter wavelengths λ is associated with a higher crack density. In contrast, a shift to longer wavelengths corresponds to an expansion of existing cracks.

Preprints (www.preprints.org) | NOT PEER-REVIEWED | Posted: 23 March 2022 doi:10.20944/preprints202203.0308.v1

2.5. Tribology and Surface Degradation

Tribology tests were performed using a custom-made tribometer with a ring on disc geometry and a contact area of 169.65 mm². In order to test the elastomers, structured and DLC coated elastomer rings (NBR-H-AT-68, $Ø_{inner}$: 9.2 mm; $Ø_{outer}$: 21 mm, thickness: 2 mm) were glued on a metal discs (AS_0821, 100Cr6) with cyano-acrylate glue and dried for one night. As counterpart axial bearings steel discs (AS_1528, 100Cr6, R_a 0.1 µm, Rz 0.8 µm, RPC 64/cm, technical roughness) were used. A load of 0.3 MPa at 148 rpm (0.14 m/s) was applied for long-time experiments under dry conditions, which lasted for 12 h. The structural development of the abraded surface area was captured using a Laser-scanning microscope Keyence VK 9700K with a step size in z-direction of 0.5 µm at 20x magnification.

3. Results

3.1. Laser Processing

All materials, independent of fillers or transparency, could be processed homogenously and consistently.

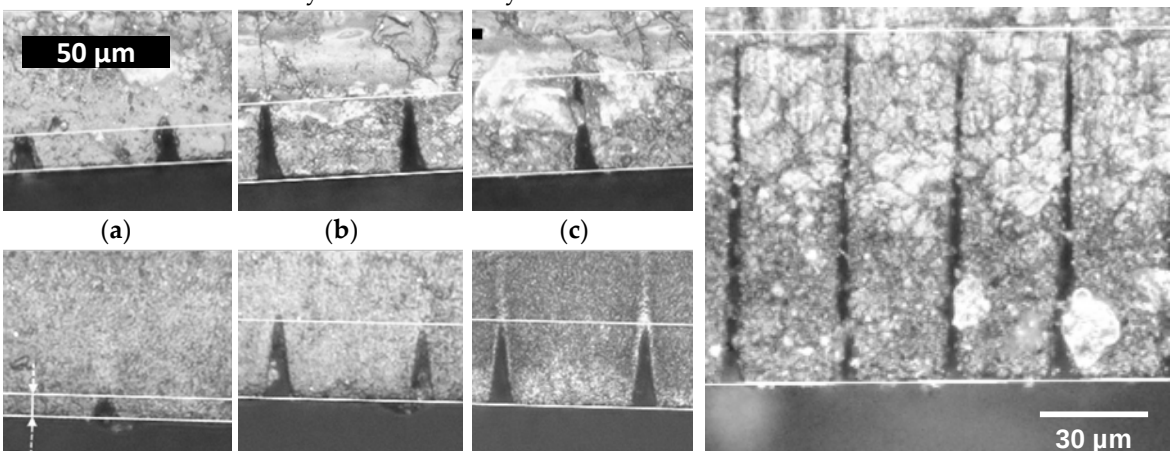

Figure 2. Comparison of SEBS G1650 (**a**)-(**c**) and NBR H-AT-68 (**d**)-(**f**) for 0.45 µJ pulse energy and 60 µm hatching. The number of repetitions is increased from left to right from 5 over 15 to 20.

A cross section of NBR and a translucent SEBS are exemplary depicted in Figure 2. Both show a similar dependency on the number of scans as indicated by the similar single shot threshold fluence (Table 1). High aspect ratio trenches (16:1) with a constant width of approximately 10 µm could be manufactured in all materials (Figure 2.g).

3.2. DLC-coating of rubber substrates

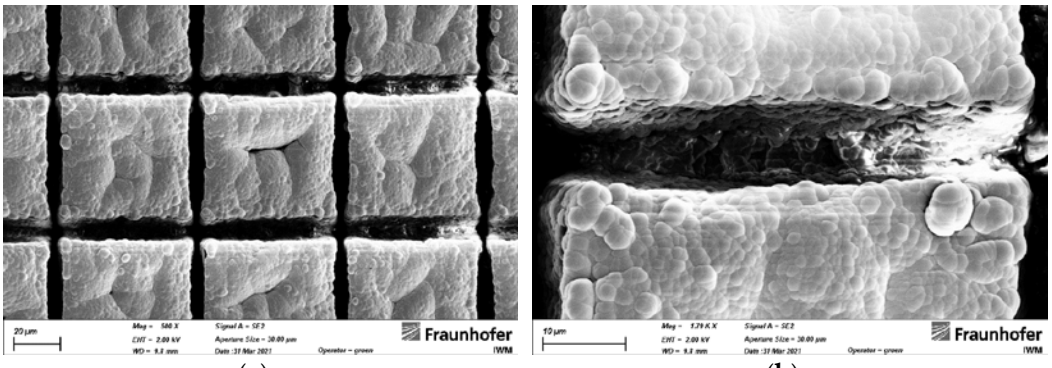

Figure 3. DLC-coating on elastomer substrate with a hatch distance of 30 µm (S30).

 doi:10.20944/preprints202203.0308.v1

The DLC coating of all rubber substrates was successful and no delamination or excessive substrate warping was detected. The DLC coating had a thickness of 2.5 µm and a Vickers micro hardness of 1350 µm. By SEM analysis, A continuous DLC-coating was identified inside the trenches and depressions.

3.3. Tensile Test

Figure 3 shows the average (n = 3) stress-strain curves for uncoated and DLC-coated FKM Viton 75, both unstructured and measured with a sample size. The elastic modulus of the uncoated sample (19.1 MPa) is lower than the elastic-modulus of the DLC-coated sample (28.9 MPa). Furthermore, the coating leads to higher tensile strength and higher elongation at break.

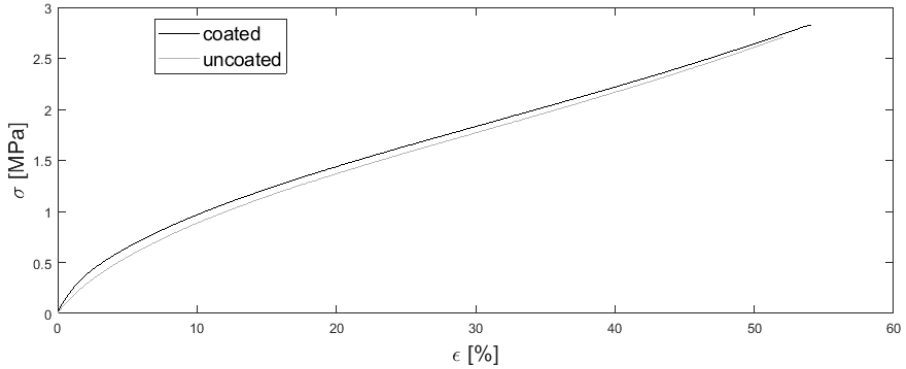

Figure 3. Stress (ε)-Strain (σ)-Diagram of uncoated and DLC-coated FKM samples.

The DLC-coating of the unstructured reference sample showed an irregular pattern of cracks with no recognizable preferred direction before elongation. According to the Fourier transformation the wavelength distribution peaks around 90 µm and 100 µm in, respectively perpendicular to the elongation direction. The DLC-coating of the sample with structure S1 shows a regular grid pattern with 60 µm spatial separation in and perpendicular to the elongation direction. Small voids and substructures are recognizable in each slab. A similar coating morphology is found for structure S2 with DLC coating. However, some slabs are connected by a continuous DLC-coating without a recognizable trench in between. Neither sample showed delamination of the DLC-coating.

Reference: At 10 % strain of the reference sample a noticeable increase of cracks is identified visually accompanied by the onset of the SPD-shift towards shorter wavelengths. Until 40 % strain an ongoing SPD-shift is observed. Further elongation shifts the SPD towards longer wavelengths. In real space, further fragmentation is not observed. However, the already existing cracks are expanded. The SPD shift asymptotically approaches the measured elongation, highlighted by the dotted line. After unloading, the cracks are completely closed and the SPD corresponds to the SPD before the tensile test.

Structure S1: Up to 34 % strain, the existing trenches in elongation direction are expanded while the trenches perpendicular to the elongation direction contract. They are become fully closed at around 34 % strain. Towards higher strains different distortion phenomenon of the slabs are observed: pincushion distortions and meandering perpendicular to the elongation direction. Cracks seem to form inside some individual slabs. The SPD is constantly shifted towards longer wavelengths. The shift follows the elongation as highlighted by the dotted line.

Preprints (www.preprints.org) | NOT PEER-REVIEWED | Posted: 23 March 2022 doi:10.20944/preprints202203.0308.v1

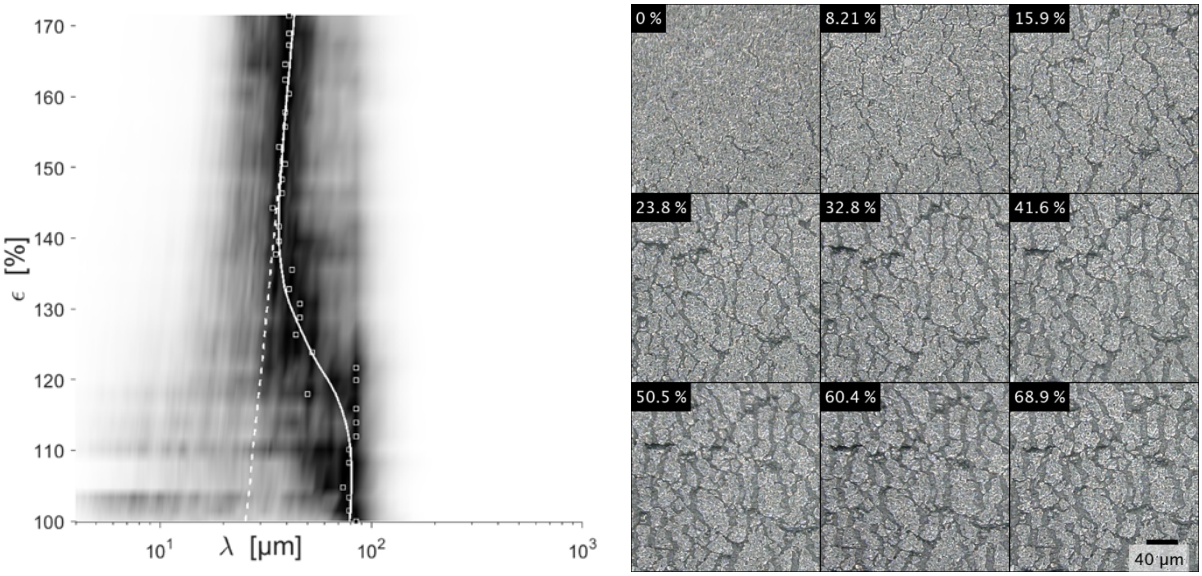

(**a**) (**b**)

Figure 4. DLC-coating on an unstructured substrate, showing the same section at different strains, (**b**) and the corresponding SPD (**a**). The dotted white line highlights the measured strain. The solid white line is a logistic curve fit to the maximum SPD values at each strain. It asymptotically approaches the measured strain. The SPD is normalized, and the contrast is enhanced by taking the fourth power. The maximum SPD value is marked by the squares.

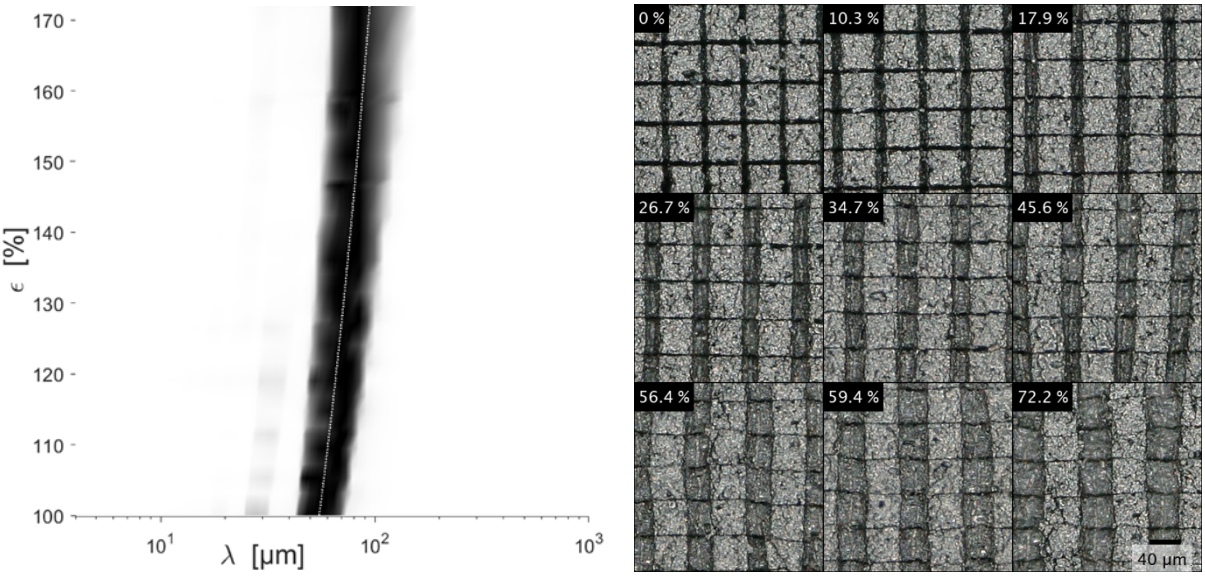

(**a**) (**b**)

Figure 5. Microscope images (real space) of strained DLC-coating with structure 1 (**b**) and the corresponding SPD (**b**). The dotted white line highlights the measured strain. The SPD is normalized, and the contrast is enhanced by taking the fourth power.

Structure S2: An inspection of the DCL-coating at 6 % strain shows an advanced expansion of some trenches in contrast to others. Further straining intensifies this irregularity which ultimately leads to meandering perpendicular to the elongation direction. The SPD peak shifts constantly towards longer wavelengths, following the elongation. Compared to S1 the SPD is broader, indicating an irregular expansion. For some samples, the DLC-coating bridged the trenches, except the trench intersections, leading to a morphology as in S3 and a similar fracture behavior as the reference sample.

Preprints (www.preprints.org) | NOT PEER-REVIEWED | Posted: 23 March 2022 doi:10.20944/preprints202203.0308.v1

3.4. Tribology and Surface Degradation

The structures S1 to S3 as well as one unstructured reference sample were investigated, each with and without DLC coating. As expected, lower friction values at the end of the test of approx. 20-30% were obtained in the tribological experiments when the elastomer is coated with DLC (Figure 6.a). This is independent of the structuring of the elastomer. Wear also decreased significantly due to the DLC coating. **Error! Reference source not found.** gives a comparison of the different structured and coated elastomer rings after the tribological experiments. The structured samples without DLC show significantly more macroscopic abrasion patterns after the tribological experiment than the unstructured sample.

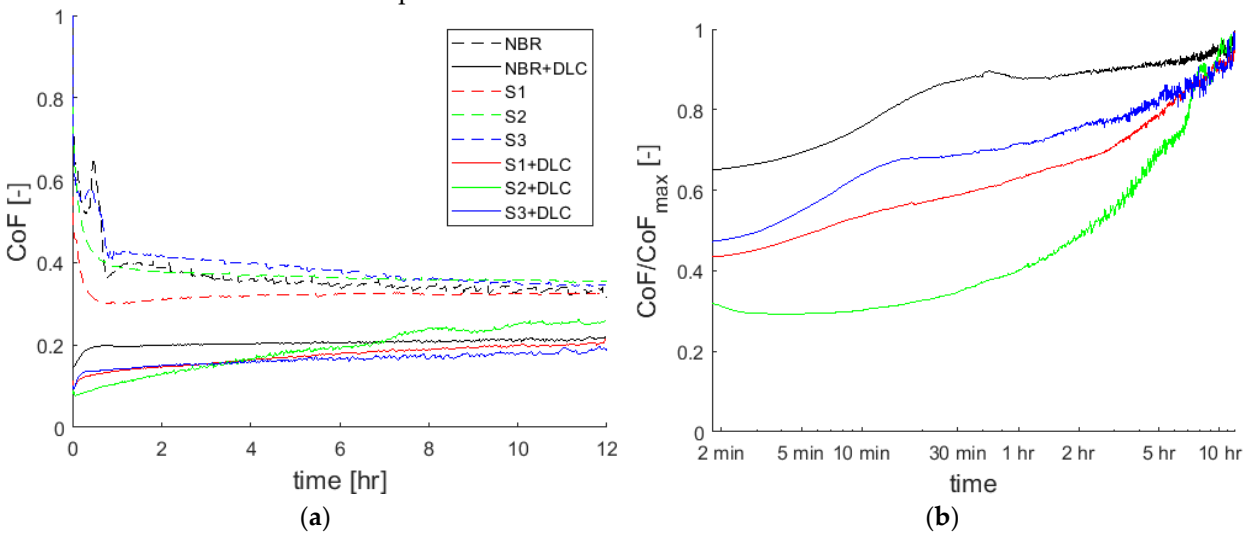

(**a**) (**b**)

Figure 6. left: Friction coefficient of different elastomer samples; right: evolution of the normalized friction coefficient for DLC-coated elastomers

The DLC coating results in a different running-in behavior of the specimens: whereas for uncoated samples typically a decreasing CoF is observed, the coated samples exhibit a continuously increasing CoF. The initial high friction ($\mu = 0.6$) occurring for the elastomer-steel contact (high adhesive contact) decreases to a run-in condition ($\mu \sim 0.35$) after about 1-2 h. The friction values of the DLC-coated elastomers start at about 0.1 and - depending on the structure - develop quickly or slowly into a steadily increasing CoF, which reaches about $\mu = 0.2$ after 12 h. For the DLC coated sample (+DLC) a very fast increase of the CoF within the first 30 min was found which then continued to increase steadily at a significantly lower rate. The CoF of the S3+DLC specimen also exhibits a very strong increase within the first 20 min. In order to facilitate the comparison of the development of the friction coefficient of the DLC-coated samples, the curves were normalized to the friction coefficient at the end of the test and plotted with a logarithmic time scale (Figure 2.b). Both, the unstructured and the point-structured samples (S3) show two regimes for the CoF: an initial increase and then a moderate increase as compared to latter. The two tile structures S1 and S2 do not show this intensive initial increase.

In the two top rows in **Error! Reference source not found.** laser scanning microscopic pictures (20x magnification) of the DLC coated surfaces before and after the tribological experiment are compared. The unstructured DLC coated surface shows initially a complex structured morphology. As a result of the tribological loading this structure becomes more fragmented. The patterns of the structured elastomer samples remain clearly visible when coated with DLC. A fragmentation of the DLC coating in the wear track (similar as for the unstructured specimen) for S3+DLC is equally noticeable. The other two DLC coatings (tile structures S1 and S2) do not show any clear change of the coating pattern.

Preprints (www.preprints.org) | NOT PEER-REVIEWED | Posted: 23 March 2022 doi:10.20944/preprints202203.0308.v1

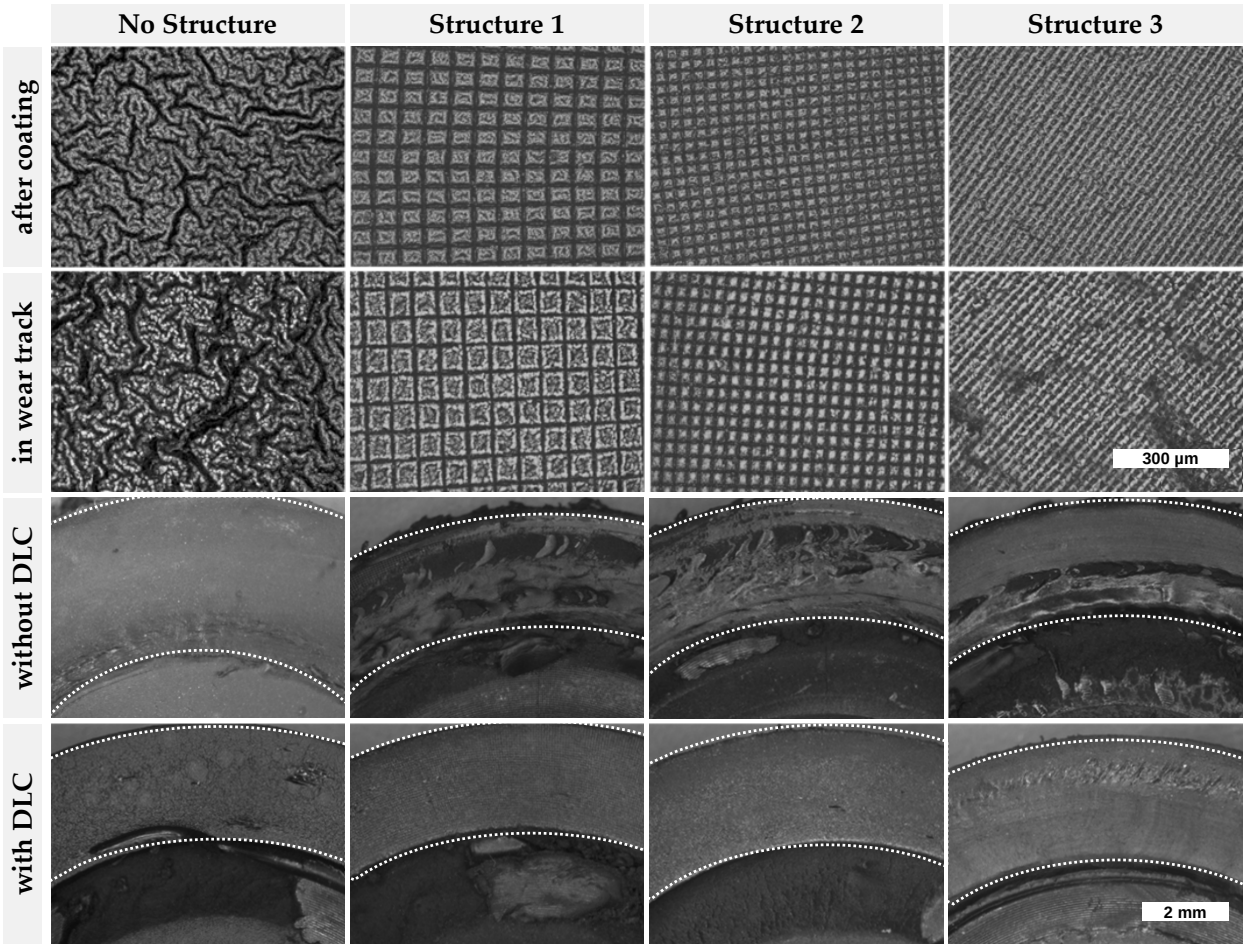

Figure 8. DLC coated surfaces before and after tribological loading.

4. Discussion

From the coating texture alone (Figure 5), the conclusion can be drawn, that the trenches facilitate stress relief inherited from the coating process. During tensile tests, the individual tiles of structure 1 and 2 experienced no further fragmentation. The induced stress is completely relieved by the expansion of the trenches. The same principal is observed for the native, unstructured coating. However, a threshold crack density needs to be surpassed. This crack density is dependent on the film adhesion, tensile strength, and film thickness [19]. Up to 8 % strain, preexisting cracks are expanded. Further straining fragments the film up to the threshold crack density at 35 % strain. These findings are in accordance with [18]. However, one load cycle does not change the SPD of the reference sample when unloaded to 0 % strain, which may indicate an insufficient resolution of the utilized optical system. Thus, the cracks observed at ca. 35 % strain may be the initially generated network, which was not resolved at 0 % strain. However, a similar analysis by Pei et al. ([18], Figure 5) indicates that the newly formed crack pattern is overshadowed by the pristine.

DLC-coated samples show a slightly higher elastic modus, tensile strength and elongation at break. Keeping inaccuracies and scattering in the measurement in mind, it can be stated that the found differences are negligible. It can be speculated that the early fragmentation of the DLC-coating (Figure 4.b) leads to no great differences in mechanical properties.

As seen in the results section, the structured uncoated elastomers show significantly higher abrasion than the unstructured sample. This can be explained by the existing pre-

 doi:10.20944/preprints202203.0308.v1

determined breaking points. This internal load results in a quicker material chipping behavior. The application of a nano-structuring could be a future improvement step. As expected, a DLC coating - regardless of the structuring - leads to a lower CoF and low wear. There are three explanations for this. First, the hysteretic friction of an elastomer-steel contact disappears with DLC coatings. Second, the bulging of the DLC layer - caused by the coating process - reduces the contact area and adhesive friction. Thirdly, the adaptability of a harder and stiffer DLC layer to the tribological partner is significantly lower than that of a softer elastomer. A closer look at the individual DLC-coated samples leads to the following conclusions: The DLC- layer on the unstructured elastomer specimen shows a cauliflower-like "wavy cap" structure. The average waviness (approx. 80 µm). of this coating is higher than the average waviness of the layers on the structured specimens During tribological loading, the protruding caps are crushed or worn and then lead to smaller fragmented still fixed coating pieces, as seen in the tensile tests. Fracture is assisted by the underlying shear stress introduced into the interfacial area by the coating. The initial small contact area at the top of the cap increases with ongoing fracture of the caps. This development is typically fast. The point structure S3 with DLC-coating also exhibits this behavior as this structure does not strongly contribute to the reduction of the stress induced by the coating process. The layer also looks fragmented after the test. The tile structures allow stress release during the coating process and the result is a more resilient surface structure. In the case of continuous loading, less heterogeneous damage is produced. The ability of the tiles to reduce shear strain during dynamic friction mitigates overloading effects. The CoF changes more steadily, and the structures do not (yet) show the larger-scale fragmentation. In this case, the development of the coating change or destruction can be observed via the CoF. The findings for short-term measurements in the way of initial damage of any cap structure and the resilience of tile structures to frictional shear load can be projected to long term behavior. The optimal limit would be found for a coated structure that only decays by DLC wear until the coating is sacrificed.

5. Conclusion and outlook

Elastomer substrates were laser microstructured with either two different tile patterns or a matrix of dimples and subsequently coated with DLC. Unstructured, DLC-coated NBR samples showed a primordial crack network after coating. Under tensile stress a further fragmentation of the DLC-coating was observed, whereas a tile patterned substrate efficiently suppressed any further cracking except in the predisposed trenches. The coated samples showed a significantly reduced CoF compared to the uncoated ones. The structuring helped in the coated as well as in the uncoated state to lower the CoF und reduce wear. This effect wore of partly over time and was dependent on the surface structure. Macroscopically, the tile patterned samples (S1 and S2) look almost unaffected after tribology tests. We associate this finding with the superior resilience of the tile-patterned coating to ongoing fragmentation. The stability of the positive effect of the CoF correlates with the stability of the structures against strain.

The positive effects of the surface structuring on the CoF, wear and especially the formation of different crack patterns open up a wide range of new developments to control the surface structure of DLC coated rubbers and to enhance the tribological performance of, for example, rubber sealings.

Author Contributions: S.V., A.B. and B.B. outlined the structure of this work. S.V. conducted laser ablation experiments and tensile tests as well as their analysis. S.V. wrote the introduction, the subchapter tensile tests. B.S. performed tribology experiments and wrote the affiliated chapters. B.B. was responsible for DLC coating and the accompanying chapter. F.K. and T.v.R performed tensile tests. S.V., B.S., F.K. and T.v.R. contributed to the discussion and S.V. and B.B. to the conclusion section.

Funding: This research received no external funding

Institutional Review Board Statement: not applicable

Informed Consent Statement: not applicable

Data Availability Statement: Data is available upon request.

Conflicts of Interest: no conflicts of interest are present.

Appendix A

The spatial frequency distribution was obtained by a two-dimensional fast Fourier transformation (2D-FFT) of microscope images. The reflectivity of cracks, DLC and substrate is different which results in a shaded image. Thus, the intensity spectrum resembles the morphology of the surface. Each image is composed from various wavelength, spanning from two pixels of length to the whole image width. The intensity distribution of the 2D-FFT reflects which wavelengths are dominant in the image. The center of the 2D-FFT represents a wavelength of infinity (the mean image intensity). Moving radially outwards, the wavelengths decreases. In order to obtain the wavelength spectrum (corresponding to the reciprocal SPD), the intensities of the 2D-FFT along each radius are averaged. Since an incrementally small increase of the radius is not feasible, the intensities are collected in bins. The spectrum is normalized by the maximum.

References

1. Pei, Y.T.; Bui, X.L.; Zhou, X.B.; Hosson, J.T.M. de. Tribological behavior of W-DLC coated rubber seals. *Surface and Coatings Technology* **2008**, *202*, 1869–1875, doi:10.1016/j.surfcoat.2007.08.013.
2. Zhang, L.; Zong, X.; Guo, F.; He, B.; Yuan, X. Effect of Fluorine Incorporation on DLC Films Deposited by Pulsed Cathodic Arc Deposition on Nitrile Butadiene Rubber and Polyurethane Rubber Substrates. *Coatings* **2020**, *10*, 878, doi:10.3390/coatings10090878.
3. Suleyman Bayrak; Dominik Paulkowski. Low Friction and Wear of Elastomers by DLC Coating. *Tribologie und Schmierungstechnik* **2020**, *67*, doi:10.30419/TuS-2020-0004.
4. Bayrak, S.; Paulkowski, D.; Stöckelhuber, K.W.; Staar, B.; Mayer, B. A Comprehensive Study about the Role of Crosslink Density on the Tribological Behavior of DLC Coated Rubber. *Materials (Basel)* **2020**, *13*, doi:10.3390/ma13235460.
5. Bui, X.L.; Pei, Y.T.; Mulder, E.D.G.; Hosson, J.T.M. de. Adhesion improvement of hydrogenated diamond-like carbon thin films by pre-deposition plasma treatment of rubber substrate. *Surface and Coatings Technology* **2009**, *203*, 1964–1970, doi:10.1016/j.surfcoat.2009.01.027.
6. Thirumalai, S.; Hausberger, A.; Lackner, J.M.; Waldhauser, W.; Schwarz, T. Effect of the type of elastomeric substrate on the microstructural, surface and tribological characteristics of diamond-like carbon (DLC) coatings. *Surface and Coatings Technology* **2016**, *302*, 244–254, doi:10.1016/j.surfcoat.2016.06.021.
7. van der Pal, J.P.; Martinez-Martinez, D.; Pei, Y.T.; Rudolf, P.; Hosson, J.T.M. de. Microstructure and tribological performance of diamond-like carbon films deposited on hydrogenated rubber. *Thin Solid Films* **2012**, *524*, 218–223, doi:10.1016/j.tsf.2012.10.005.
8. Thirumalai, S.; Hausberger, A.; Lackner, J.M.; Waldhauser, W.; Schwarz, T. Anode layer source plasma-assisted hybrid deposition and characterization of diamond-like carbon coatings deposited on flexible substrates. *Thin Solid Films* **2018**, *655*, 54–61, doi:10.1016/j.tsf.2018.04.012.
9. Pei, Y.T.; Bui, X.L.; van der Pal, J.P.; Martinez-Martinez, D.; Hosson, J.T.M. de. Flexible diamond-like carbon film coated on rubber. *Progress in Organic Coatings* **2013**, *76*, 1773–1778, doi:10.1016/j.porgcoat.2013.05.015.
10. Pei, Y.T.; Martinez-Martinez, D.; Hosson, J.T.M. de. Flexible DLC film coated rubber: friction and the effect of viscoelastic deformation of rubber substrate. In *Surface Effects and Contact Mechanics XI.* CONTACT AND SURFACE 2013, Siena, Italy, 05–07 Jun. 2013; Hosson, J.T.M. de, Brebbia, C.A., Eds.; WIT PressSouthampton, UK, 2013; pp 145–156.
11. Bai, C.; Gong, Z.; An, L.; Qiang, L.; Zhang, J.; Yushkov, G.; Nikolaev, A.; Shandrikov, M.; Zhang, B. Adhesion and friction performance of DLC/rubber: The influence of plasma pretreatment. *Friction* **2021**, *9*, 627–641, doi:10.1007/s40544-020-0436-6.
12. Martinez Martinez, D. Protection of elastomers with DLC film: deposition, characterization and performance. Dissertation; University of Groningen, Groningen, 2017.
13. Aoki, Y.; OHTAKE, N. Tribological properties of segment-structured diamond-like carbon films. *Tribology International* **2004**, *37*, 941–947, doi:10.1016/j.triboint.2004.07.011.
14. Hutchinson, J.W.; Suo, Z. Mixed Mode Cracking in Layered Materials. *Advances in Applied Mechanics Volume 29*; Elsevier, 1991; pp 63–191, ISBN 9780120020294.
15. Moon, M.-W.; Lee, K.-R.; Oh, K.H.; Hutchinson, J.W. Buckle delamination on patterned substrates. *Acta Materialia* **2004**, *52*, 3151–3159, doi:10.1016/j.actamat.2004.03.014.
16. Stafford, C.M.; Harrison, C.; Beers, K.L.; Karim, A.; Amis, E.J.; VanLandingham, M.R.; Kim, H.-C.; Volksen, W.; Miller, R.D.; Simonyi, E.E. A buckling-based metrology for measuring the elastic moduli of polymeric thin films. *Nat. Mater.* **2004**, *3*, 545–550, doi:10.1038/nmat1175.

17. Faruque Ahmed, S.; Nagashima, S.; Lee, J.Y.; Lee, K.-R.; Kim, K.-S.; Moon, M.-W. Self-assembled folding of a biaxially compressed film on a compliant substrate. *Carbon* **2014**, *76*, 105–112, doi:10.1016/j.carbon.2014.04.056.
18. Pei, Y.T.; Bui, X.L.; van der Pal, J.P.; Martinez-Martinez, D.; Zhou, X.B.; Hosson, J.T.M. de. Flexible diamond-like carbon films on rubber: On the origin of self-acting segmentation and film flexibility. *Acta Materialia* **2012**, *60*, 5526–5535, doi:10.1016/j.actamat.2012.07.017.
19. Ollivier, B.; Dowey, S.J.; Young, S.J.; Matthews, A. Adhesion assessment of DLC films on PET using a simple tensile tester: Comparison of different theories. *Journal of Adhesion Science and Technology* **1995**, *9*, 769–784, doi:10.1163/156856195X00662.